

000
001
002
003
004
005
006
007
008
009
010
011
012
013
014
015
016
017
018
019
020
021
022
023
024
025
026
027
028
029
030
031
032
033
034
035
036
037
038
039
040
041
042
043
044
045
046
047
048
049
050
051
052
053054
055
056
057
058
059
060
061
062
063
064
065
066
067
068
069
070
071
072
073
074
075
076
077
078
079
080
081
082
083
084
085
086
087
088
089
090
091
092
093
094
095
096
097
098
099
100
101
102
103
104
105
106
107

Guided Proofreading of Automatic Segmentations for Connectomics

Supplemental Material

Anonymous ICCV submission

Paper ID 0922

	Traditional Network		Residual Network	
Conv. Layers	2	4	5	13
Dropout Reg.	y	y	y	n
Cost [m]	27.5	383	5080	1094
Test. Acc.	0.925	0.94	0.93	0.90
Prec./Recall	0.93/0.93	0.94/0.94	0.7/0.53	0.74/0.66
F1 Score	0.93	0.94	0.39	0.64
		*		

Table 1: Traditional CNN Architecture versus Residual Network Architecture [1]. All configurations are compared using the same parameters. Our final choice (indicated by *) trains relatively fast and performs better.

Parameter	Search Space
Filter size:	3x3, 5x5, 9x9, 13x13
No. Filters 1:	32, 48, 64
No. Filters 2-4:	32, 48 , 64
Dense units:	256, 512
Learning rate:	0.00001, 0.0001, 0.001, 0.01, 0.03-0.00001
Momentum:	0.9, 0.95, 0.9-0.999
Mini-Batchsize:	10, 100, 128

Table 2: Brute force parameter search for the split error classifier. The final parameters are highlighted.

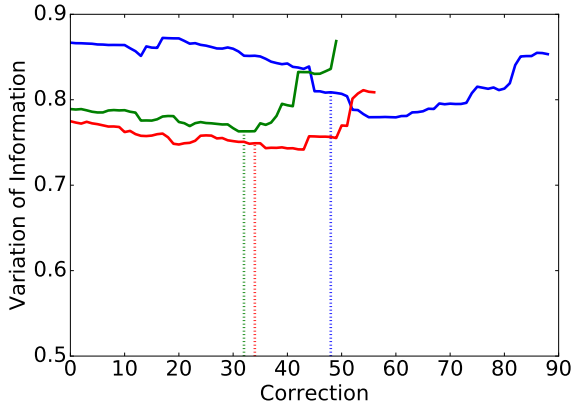


Figure 1: Observations of probability thresholds p_t during automatic selection on three different subvolumes of previously unseen testing data. The dashed lines show when $p_t = 0.95$ is reached.

1. Classifier

1.1. Architecture

We explored different architectures for the convolutional neural network (CNN) for split error detection. We compare traditional CNN architectures versus residual networks [1] (Tab. 1). The traditional architecture with dropout regularization generalized better than residual networks on unseen testing data.

1.2. Training Parameters

We performed a limited brute force parameter search to tune the split error classifier (Tab. 2). This resulted in 3240 different CNN configurations which were evaluated on 10% of our training data. Learning rate and momentum ranges are defined linearly across 2000 epochs.

1.3. Automatic Method Threshold p_t

For automatic selection, we observed a threshold $p_t = 0.95$ as stable when evaluating on previously unseen testing data (Mouse S1 AC3 Open Connectome Project dataset). This means that automatic selection stops once all borders with $p_t \geq 0.95$ were proofread. Figure 4 shows split error

classification on three randomly selected subvolumes ($700 \times 700 \times 2$ voxels) of AC3. In all cases, the threshold $p_t = 0.95$ reduces VI.

108	Algorithm 1 Merge Error Detection for a label l	162
109	1: $l_d = \text{dilate}(l, 20)$	163
110	2: $\text{invImage} = \text{invert}(\text{image})$	164
111	3: for N iterations do	165
112	4: $s_1, s_2 = \text{randomSeedsOnBoundary}(l_d)$	166
113	5: $\text{wsImage} = \text{watershed}(\text{invImage}, l_d, s_1, s_2)$	167
114	6: $\text{border} = \text{border}(\text{wsImage})$	168
115	7: $p = \text{rank}(\text{border})$	169
116	8: $p_{\text{merge}} = 1 - p$	170
117	9: find (max p_{merge})	171
118		172
119		173
120		174

1.4. Merge Error Detection Pseudo Code

1.5. Limitations

124 Guided proofreading works on 2D image sections. This
125 enables error correction without a computationally expensive
126 alignment process. However, the output requires an additional (block-)merging step prior to 3D analysis. Several
127 software packages exist for this purpose.

128 As described in Section 4, the guided proofreading classifier
129 has to be retrained if used on a different species than mouse. In our experiments, parameters did not need to be
130 changed.

2. Automatic Segmentation Pipeline

134 We create a dense automatic segmentation of electron
135 microscopy data using a combination of a U-net [5] and
136 the GALA agglomeration method [3]. These classifiers are
137 trained on different data than GP (Tab. 3).

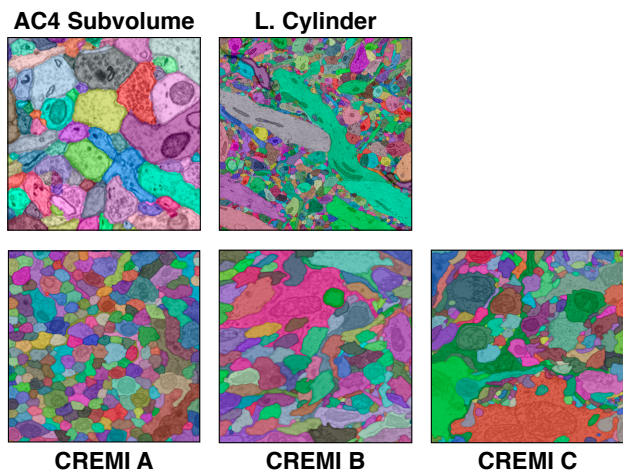
Training Set U-Net / GALA	Training Set GP	Test Set GP
AC3+AC4 (1024 × 1024 × 175vx)	L. Cylinder (2048 × 2048 × 250vx)	L. Cylinder _{test} (2048 × 2048 × 50vx)
AC4 excl. test (1024 × 1024 × 90vx)	L. Cylinder (2048 × 2048 × 250vx)	AC4 _{test} subvolume (400 × 400 × 10vx)
AC3+AC4 (1024 × 1024 × 175vx)	CREMI A/B/C (1250 × 1250 × 300vx)	CREMI A/B/C _{test} (1250 × 1250 × 15vx)

148 Table 3: Training data of membrane detection (U-Net /
149 GALA) vs. training data of GP vs. test data.

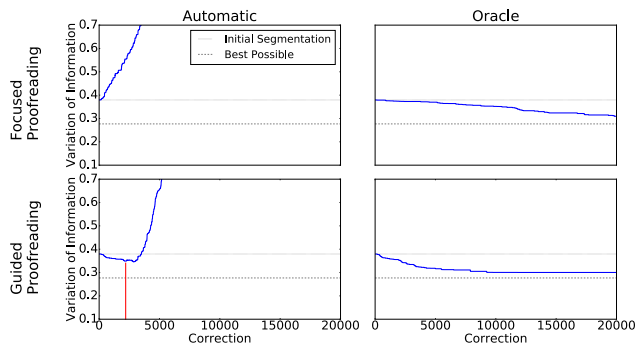
151 GALA uses a random forest classifier to agglomerate
152 segments. We use an agglomeration level of 0.3 (after a grid
153 search). Further details of our pipeline are described in [2].

3. L. Cylinder Results

157 We report experiments and results on the L. Cylinder
158 dataset in the paper. Figure 3 and 4 visualize the reported
159 results measured as variation of information (VI). We
160 compare automatic selection with threshold and selection oracle
161 using focused proofreading and guided proofreading.



172 Figure 2: The five different datasets we use for evaluation.
173 The top row shows the first slice of the AC4 and L. Cylinder
174 mouse brain datasets as reported in the paper. The bottom
175 row shows the first slice of the CREMI A/B/C fruit fly
176 datasets which we used for additional experiments.



178 Figure 3: Performance comparison of Plaza’s focused proof-
179 reading and our guided proofreading on the L. Cylinder
180 dataset as reported in the paper. All measurements are shown
181 as median VI, the lower the better. We compare automatic
182 selection with threshold ($p_t = 0.95$, red line) and the selec-
183 tion oracle for accepting or rejecting corrections using each
184 method. Guided proofreading yields better results faster with
185 fewer corrections.

196 **Best possible VI.** The selection oracle using guided proof-
197 reading does not reach the best possible VI score. We cal-
198 culate this score by intersecting the initial segmentation and
199 the ground truth. In theory, the classifier should be able to
200 reach this lower bound. However, due to the classifica-
201 tion patch size, the membrane probability maps we used included
202 a 30 pixel frame region. Guided proofreading ignores all
203 segments within this frame region, and so cannot reach the
204 best possible VI in some datasets.

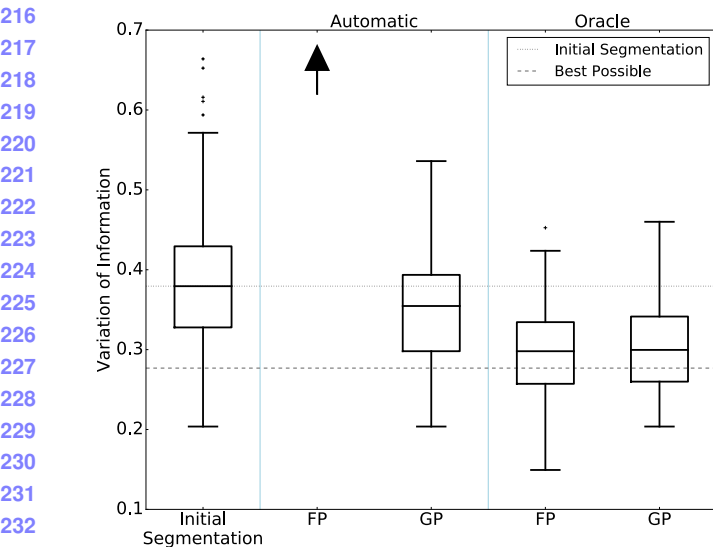


Figure 4: VI distributions of guided proofreading (GP) and focused proofreading (FP) output across slices of the L. Cylinder dataset, with different error correction approaches. The variation resulting from performance of FP with automatic selection is $7.8 \times$ higher than GP (as indicated by the arrow), with median VI of 2.75 and $SD = 0.789$.

4. Additional Experiments

CREMI A/B/C. As part of the MICCAI 2016 challenge on circuit reconstruction from electron microscopy images (CREMI), six ssTEM datasets were made publicly available¹, each $1250 \times 1250 \times 125$ voxels. Since only three datasets include manually-labeled ‘ground truth’, we use these three volumes for our experiments. The volumes are part of an adult fruit fly (*Drosophila melanogaster*) brain. The resolution of all three datasets is $4 \times 4 \times 40$ nm³/voxel. We evaluate error detection and correction on subvolumes of CREMI A/B/C with the dimensions $1250 \times 1250 \times 5$ voxels. The subvolumes were cut from the last 25 sections of each of the three datasets and unseen during training. We compare focused proofreading and guided proofreading with automatic selection ($p_t = 0.95$) and selection oracle.

Retraining. Since the CREMI data is a different species, we simply retrain our split error classifier as well as focused proofreading by Plaza [4]. For this, we use the first 100 sections of each of the three CREMI datasets combined as training data. All parameters are unchanged and left as reported in the paper.

4.1. CREMI A

Figure 5 and 6 compare Plaza’s focused proofreading and guided proofreading on the 5 sections of the CREMI A

¹<http://www.creml.org>

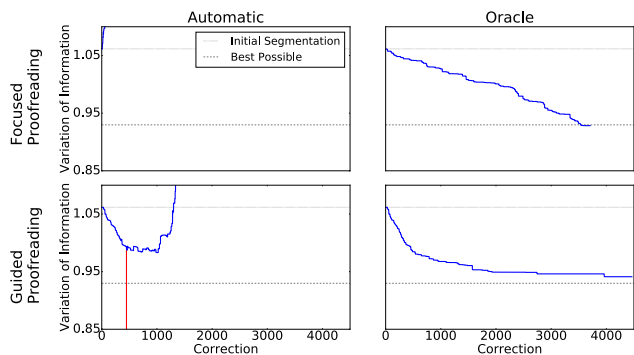


Figure 5: Performance comparison of Plaza’s focused proofreading and our guided proofreading on 5 sections of the CREMI A dataset. All measurements are reported as median VI, the lower the better. The threshold for automatic selection is $p_t = 0.95$ (red line). The slope of the selection oracle shows that guided proofreading reduces VI faster.

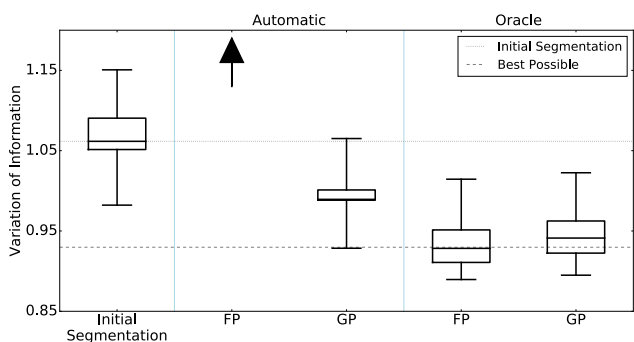


Figure 6: VI distributions of guided proofreading (GP) and focused proofreading (FP) output across slices of the CREMI A dataset, with different error correction approaches. The variation resulting from performance of FP with automatic selection is $5.4 \times$ higher than GP (as indicated by the arrow), with median VI of 5.32 and $SD = 0.009$. GP does not reach the best possible VI as discussed in the text.

dataset.

Selection oracle. With focused proofreading, the selection oracle reduces median VI to 0.928, $SD = 0.043$ from an initial median VI of 1.06 ($SD = 0.055$). 532 corrections out of 3707 were accepted. Guided proofreading does not reach the best possible VI, however, reduces VI faster with less corrections to 0.941 ($SD = 0.04$). Out of 4463 corrections, 1275 were accepted.

Automatic selection with threshold. Not surprisingly, focused proofreading performs poorly when ran automatically (VI of 5.32, $SD = 0.009$). Guided proofreading is able to reduce VI to 0.989 ($SD = 0.043$) with $p_t = 0.95$.

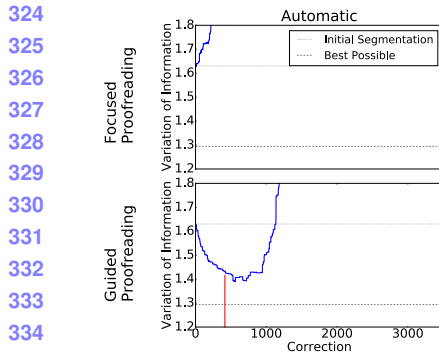


Figure 7: Split error correction by Plaza’s focused proofreading and our guided proofreading compared on the CREMI B dataset. All measurements are reported as median VI, the lower the better. Automatic selection with threshold (red line) yields reasonable performance using guided proofreading.

4.2. CREMI B

Figure 7 and 8 show the results on the CREMI B dataset.

Selection oracle. Focused proofreading is able to reduce median VI to 1.29, $SD = 0.031$ from an initial median VI of 1.63 ($SD = 0.025$). Out of 1959 corrections, the selection oracle accepted 517. With guided proofreading, the median VI is reduced to 1.30, $SD = 0.03$ while accepting 1111 corrections out of 3073.

Automatic selection with threshold. Focused proofreading results in a VI of 4.25 ($SD = 0.07$). Guided proofreading reduces median VI to 1.43 ($SD = 0.038$).

4.3. CREMI C

The results of split error correction using focused proofreading and guided proofreading on the CREMI C subvolume are shown in Figure 9 and 10.

Selection oracle. With focused proofreading, the initial median VI of 1.75 ($SD = 0.086$) is reduced to 1.45 ($SD = 0.056$) with 670 accepted corrections out of 2694. Guided proofreading is able to reduce the VI to 1.47 ($SD = 0.06$). Here, the oracle accepted 1531 out of 4332 corrections.

Automatic selection with threshold. Focused proofreading results in a VI of 4.81 ($SD = 0.03$). Guided proofreading with $p_t = 0.95$ reduces median VI to 1.57 ($SD = 0.081$).

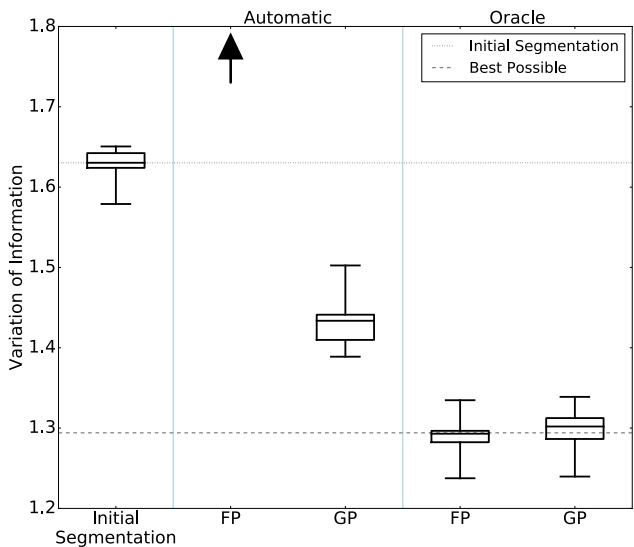


Figure 8: VI distributions of guided proofreading (GP) and focused proofreading (FP) output across 5 sections of the CREMI B dataset. We compare automatic selection and oracle selection. The variation resulting from performance of FP with automatic selection is 3× higher than GP (as indicated by the arrow), with median VI of 4.25 and $SD = 0.07$.

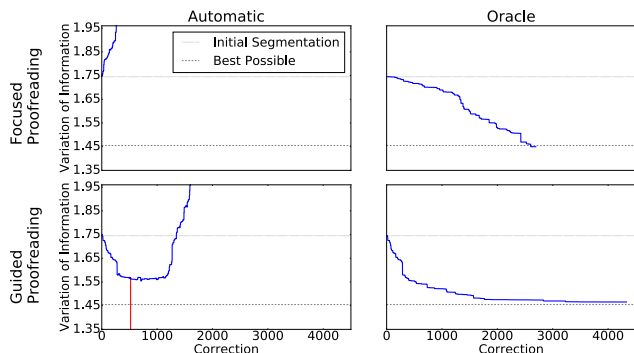


Figure 9: Performance comparison of Plaza’s focused proofreading and our guided proofreading on the CREMI C dataset. Lower VI scores are better. Guided proofreading corrects the initial segmentation faster with less corrections than focused proofreading.

5. Forced Choice User Experiment

5.1. Recruitment and Participation

Novice participants were recruited via flyer (figure 11). An anonymized listing of all participants including demographic information is shown in table 4.

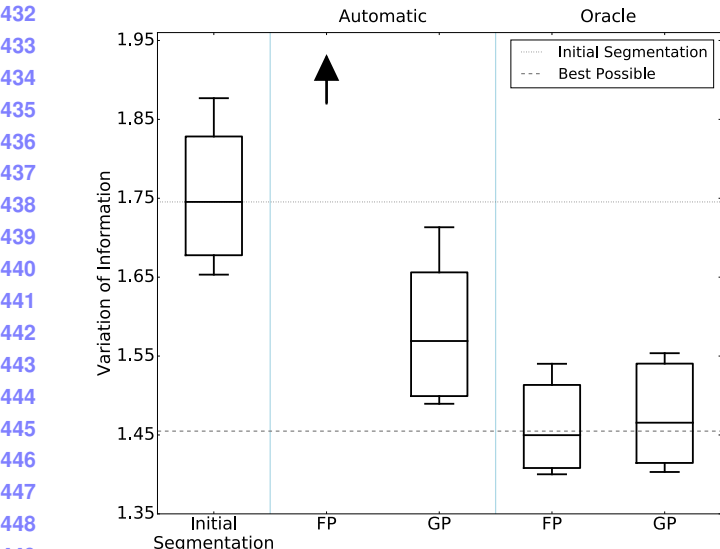


Figure 10: VI distributions of guided proofreading (GP) and focused proofreading (FP) output across the CREMI C subvolume, with different error correction approaches. The variation resulting from performance of FP with automatic selection is 3× higher than GP (as indicated by the arrow), with median VI of 4.81 and $SD = 0.08$.

ID	Sex	Age	Classifier
S38	F	20	FP
S57	F	30	FP
S32	M	38	FP
S34	F	21	FP
S21	F	65	FP
S9	M	33	FP
S45	M	28	FP
S31	M	27	FP
S24	F	21	FP
S6	F	38	FP
S28	M	32	GP
S36	F	19	GP
S35	M	26	GP
S25	M	26	GP
S54	F	30	GP
S53	M	29	GP
S52	M	27	GP
S51	M	31	GP
S200	F	37	GP
S3	F	30	GP

Table 4: The novice participants ($N = 20$) of the forced choice user experiment. The table shows sex (20 female), age ($M = 30$) and the randomly assigned classifier (focused proofreading as FP, guided proofreading as GP).



Get **\$10** Cash!
And look at
Pretty Pictures
of the brain while
helping to **Advance**
Science

We are looking for people who are 18+ and have no experience with nano-scale electron microscopy data of neurons (noobs).

The experiment will last less than 1 hour.

Starting NOW!

SIGN UP:
<http://XXX/YYXXXXXXZZZZ>

Contact: Anon. <anon@anon>
Anon.

Figure 11: Participants were recruited with this flyer.

5.2. Example Classifications

During the user study, participants were asked to accept or reject potential errors and their corrections — some more difficult than others. Figure 13 shows a selection of potential errors and their corrections.

5.3. Subjective Responses

After the experiment, we acquired subjective responses using the NASA-TLX task load index (figure 12). We performed ANOVA to test for statistical significance [6]. Mental, physical, and temporal demands were reported slightly higher for participants using focused proofreading but the analysis did not yield any significance.

- **Mental Demand.** Participants using focused proofreading stated a higher mental demand $M = 11.5$ ($SD = 2.098$) than with guided proofreading $M = 8.1$ ($SD = 2.003$). This was not statistically significant ($F_{1,18} = 3.2574, p = 0.3695$).

- **Physical Demand.** While naturally physical demand was rated low, participants using focused proofreading stated it slightly higher $M = 5.4$ ($SD = 2.26$) than with guided proofreading $M = 2.9$ ($SD = 1.76$). This

540 NASA Task Load Index

Hart and Staveland's NASA Task Load Index (TLX) method assesses work load on five 7-point scales. Increments of high, medium and low estimates for each point result in 21 gradations on the scales.

Figure 12: The NASA-TLX workload index to record subjective responses.

was not statistically significant ($F_{1,18} = 1.7507, p = 0.5454$).

- **Temporal Demand.** For temporal demand, participants using focused proofreading $M = 8.4$ ($SD = 1.95$) reported almost equal to guided proofreading $M = 8.3$ ($SD = 1.99$). This was not statistically significant ($F_{1,18} = 0.0033, p = 0.9987$).
 - **Performance.** Here, participants were asked to rate their own performance. All participants rated their performance as pretty well (the lower, the better). For focused proofreading $M = 6.8$ ($SD = 1.97$) and for guided proofreading $M = 7.8$ ($SD = 2.04$). This was not statistically significant ($F_{1,18} = 0.3091, p = 0.8878$).

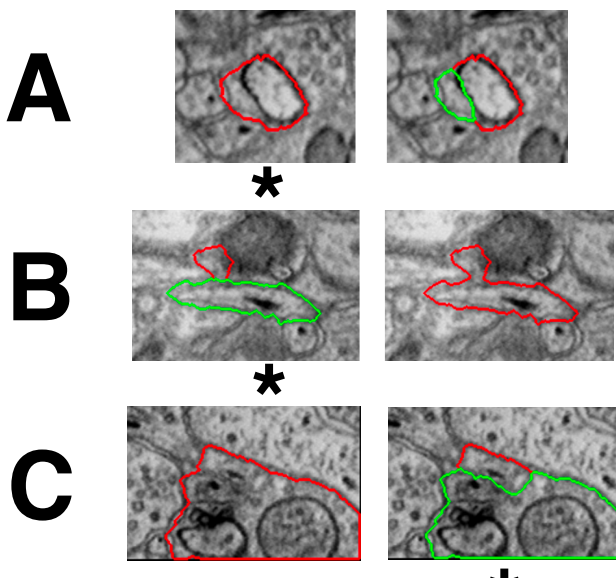


Figure 13: A selection of suggested errors and potential corrections during the forced choice user experiment. The star (*) indicates which choice reduces VI. While all participants were able to correctly choose for patch A, only few were able to correctly choose for patch B and C.

- **Effort.** Participants using focused proofreading stated higher effort $M = 13.0$ ($SD = 2.336$) than with guided proofreading $M = 10.6$ ($SD = 2.127$). This was not statistically significant ($F_{1,18} = 1.1459, p = 0.6599$).
 - **Frustration.** Participants overall reported low frustration. Reported were $M = 5.0$ ($SD = 1.90$) using focused proofreading and $M = 5.9$ ($SD = 1.85$) using guided proofreading. This was not statistically significant ($F_{1,18} = 0.3271, p = 0.8818$).

References

- [1] K. He, X. Zhang, S. Ren, and J. Sun. Deep residual learning for image recognition. In *The IEEE Conference on Computer Vision and Pattern Recognition (CVPR)*, June 2016. 1
 - [2] S. Knowles-Barley, V. Kaynig, T. R. Jones, A. Wilson, J. Morgan, D. Lee, D. Berger, N. Kasthuri, J. W. Lichtman, and H. Pfister. Rhoanet pipeline: Dense automatic neural annotation, 2016. (available on arXiv:1611.06973 [cs.CV]). 2
 - [3] J. Nunez-Iglesias, R. Kennedy, S. M. Plaza, A. Chakraborty, and W. T. Katz. Graph-based active learning of agglomeration (gala): a python library to segment 2d and 3d neuroimages. *Frontiers in neuroinformatics*, 8, 2014. 2
 - [4] S. M. Plaza. *Focused Proofreading to Reconstruct Neural Connectomes from EM Images at Scale*, pages 249–258. Springer International Publishing, Cham, 2016. 3

648	[5] O. Ronneberger, P. Fischer, and T. Brox. U-net: Convolutional	702
649	networks for biomedical image segmentation. In <i>Medical Im-</i>	703
650	<i>age Computing and Computer-Assisted Intervention (MICCAI)</i> ,	704
651	volume 9351 of <i>LNCS</i> , pages 234–241. Springer, 2015. (avail-	705
652	able on arXiv:1505.04597 [cs.CV]).	706
653	2	
654	[6] J. P. Shaffer. Multiple hypothesis testing. <i>Annual Review of</i>	707
655	<i>Psychology</i> , 46(1):561–584, 1995.	708
656	5	
657		709
658		710
659		711
660		712
661		713
662		714
663		715
664		716
665		717
666		718
667		719
668		720
669		721
670		722
671		723
672		724
673		725
674		726
675		727
676		728
677		729
678		730
679		731
680		732
681		733
682		734
683		735
684		736
685		737
686		738
687		739
688		740
689		741
690		742
691		743
692		744
693		745
694		746
695		747
696		748
697		749
698		750
699		751
700		752
701		753
		754
		755